British Journal of Pharmacology

DOI:10.1111/bph.12355
www.brjpharmacol.org

RESEARCH PAPER

Bleomycin induces endothelial mesenchymal transition through activation of mTOR pathway: a possible mechanism contributing to the sclerotherapy of venous malformations

Wei Zhang[1,2]*, Gang Chen[1,2]*, Jian-Gang Ren[1] and Yi-Fang Zhao[2]

[1]*The State Key Laboratory Breeding Base of Basic Science of Stomatology and Key Laboratory of Oral Biomedicine Ministry of Education, School and Hospital of Stomatology, Wuhan University, Wuhan, China, and* [2]*Department of Oral & Maxillofacial – Head & Neck Oncology, School and Hospital of Stomatology, Wuhan University, Wuhan, China*

Correspondence
Mr Yi-Fang Zhao, The State Key Laboratory Breeding Base of Basic Science of Stomatology and Key Laboratory of Oral Biomedicine Ministry of Education, School and Hospital of Stomatology, Wuhan University, Wuhan 430079, China. E-mail: yifang@whu.edu.cn.

*Wei Zhang and Gang Chen contributed equally to this work.

Keywords
bleomycin; endothelial mesenchymal transition; mTOR; Slug; venous malformation

Received
5 May 2013
Revised
29 July 2013
Accepted
19 August 2013

BACKGROUND AND PURPOSE

Bleomycin (BLM), one of the most common sclerosants, is often used to treat venous malformations (VMs). The present study was designed to investigate whether endothelial mesenchymal transition (EndoMT) contributes to the therapeutic effects of BLM.

EXPERIMENTAL APPROACH

Endothelial and mesenchymal markers of HUVECs were measured by immunofluorescence, real-time quantitative PCR and Western blot analysis. Cell migration and tube formation assays were performed to evaluate endothelial cell function. Slug small-interfering RNA and specific inhibitors [Z-VAD-FMK for pan caspases, rapamycin for mammalian target of rapamycin (mTOR)] were used to investigate the mechanism.

KEY RESULTS

Long term (48 h or longer) treatment with BLM (0.1 mU·mL^{-1}) induced EndoMT in HUVECs, as manifested by a reduction in the expression of vascular endothelial-cadherin and an up-regulation in the expression of α-smooth muscle actin and fibroblast specific protein-1, as well as activation of the transcription factor Slug. The size and protein content of the transformed cells were increased. BLM also enhanced the migration of HUVECs but diminished their tube formation. By employing rapamycin, we demonstrated that activation of the mTOR pathway is involved in BLM-induced EndoMT in HUVECs.

CONCLUSIONS AND IMPLICATIONS

Our results show that a Slug-dependent EndoMT process is involved in BLM-induced therapeutic effects on endothelial cells and, more importantly, indicate the potential role of this process in the sclerotherapy of VMs.

Abbreviations

α-SMA, α-smooth muscle actin; EndoMT, endothelial mesenchymal transition; FSP-1, fibroblast specific protein-1; mTOR, mammalian target of rapamycin; siRNA, small-interfering RNA; VE-cadherin, vascular endothelial-cadherin; VMs, venous malformations

Introduction

Venous malformations (VMs) are the most frequent slow-flow vascular malformations, which are composed of dilated and serpiginous channels (Wouters *et al.*, 2010). Pharyngeal or laryngeal VMs can compromise the airways of individuals and cause snoring, and even sleep apnoea (McRae *et al.*, 2013). They can also be life-threatening as they may bleed, expand or obstruct vital structures (McRae *et al.*, 2013). The current treatments for VMs include surgical resection, laser therapy and sclerotherapy (Dompmartin *et al.*, 2010; McRae *et al.*, 2013). Based on the specific histological characteristics, represented as enlarged venous channels lined by a single flattened layer of endothelial cells surrounded by sparse smooth muscle cells, intralesional sclerotherapy is now widely accepted as the preferred treatment to diminish the volume of the disease (Odeyinde *et al.*, 2013).

Bleomycin (BLM) is a gentle and effective sclerosant and has been widely used to treat vascular malformations, including VMs (Muir *et al.*, 2004). The underlying mechanism of BLM-induced sclerotherapy was traditionally considered to be the obliteration of enlarged channels induced by endothelium damage as a result of acute or chronic inflammation and fibrosis (Yamamoto and Katayama, 2011). However, evidence is now emerging that treatment with BLM affects the adhesion molecules of the endothelium and destroys intercellular interactions (Horikawa *et al.*, 2006; Ohta *et al.*, 2012). In addition, it has been found that the expression levels of tight junction proteins in endothelial and alveolar epithelial cells are down-regulated during BLM-induced lung injury (Ohta *et al.*, 2012). However, the precise mechanisms underlying the above changes induced by BLM still need to be clarified.

BLM is also a common inducer of fibrosis and has been frequently used for establishing models of pulmonary fibrosis (Harrison and Lazo, 1987; Mouratis and Aidinis, 2011). Notably, in a recent study it was found that the pulmonary endothelial cells within a BLM-induced pulmonary model had undergone distinct morphological changes, which were further identified as endothelial mesenchymal transition (EndoMT) (Hashimoto *et al.*, 2010). EndoMT is a process by which endothelial cells lose their polarities and cobblestone-like morphologies, and change into fibroblast-like cells, express fibroblast proteins and lose their intrinsic endothelial markers, such as CD31 and vascular endothelial (VE)-cadherin (Arciniegas *et al.*, 2005; Zeisberg *et al.*, 2007). The process is similar to epithelial mesenchymal transition (EMT), which is a common phenomenon during development and tumorigenesis (Thiery *et al.*, 2009). It has been demonstrated that both EndoMT and EMT are usually regulated by two types of transcription factors, the basic helix-loop-helix transcription factors, which include E12/E47 and twist, and the zinc finger transcription factors, which include Snail, Slug, Zeb1 and Zeb2 (also called SIP1) (Piera-Velazquez *et al.*, 2011).

In the present study, we showed that continuous treatment with BLM induced changes in endothelial cells that appeared to be EndoMT. Additionally, our data also suggest that the transformation induced by BLM was regulated by the EMT-related transcription factor Slug in an Akt/mammalian target of rapamycin (mTOR) pathway-dependent manner. Most importantly, up-regulated expression of Slug was also detected in human BLM-treated VM specimens. Collectively, our results show that Slug-dependent EndoMT is involved in BLM-induced therapeutic effects on endothelial cells and, more importantly, indicate its potential role in the sclerotherapy of VMs.

Methods

Regents and antibodies

Culture media and buffers were purchased from Gibco (Carlsbad, CA, USA). BLM and rapamycin were purchased from Sigma-Aldrich (St. Louis, MO, USA). Z-VAD-FMK was purchased from Merck (Darmstadt, Germany). Primary antibodies against Akt, phosphorylated Akt, mTOR, phosphorylated mTOR, S6, phosphorylated S6, cleaved-caspase 3, VE-cadherin and Slug were purchased from Cell Signaling Technology (Danvers, MA, USA). Primary antibodies against α-smooth muscle actin (α-SMA) and fibroblast specific protein-1 (FSP-1) were purchased from Epitomics (Burlingame, CA, USA). Primary antibodies against CD34 and GAPDH were obtained from Santa Cruz Biotechnology, Inc. (Santa Cruz, CA, USA). For small-interfering RNA (siRNA)-mediated inhibition, siRNA sequences against human Slug (5′-CAGACCCATTCTGATGTAAAG-3′) were cloned into pBRsi-hU6 lentiviral vector systems. The negative control siRNA and lentiviral vector package were provided by Genechem (Shanghai, China). The RNA interference efficiency has been confirmed in our previous study (Jia *et al.*, 2012).

Cell culture

HUVECs were isolated from human umbilical cord veins by collagenase treatment as previously described (Zou *et al.*, 2013). HUVECs were cultured in endothelial basal medium (EBM; Cambrex Bio Science, Walkersville, MD, USA) supplemented with 20% fetal bovine serum, SingleQuot (Cambrex Bio Science), and penicillin-streptomycin-fungizone mixture. The cells in the present study were used in passages 2–7. Cell volume was measured by the Vi-CELL cell viability analyser (Beckman Coulter, Fullerton, CA, USA), and cell content was measured by bicinchoninic acid (BCA) protein assay kit (Pierce Chemical, Rockford, IL, USA) according to the manufacturer's recommendations.

Clinical samples and immunohistochemistry

Twenty VMs (including 10 cases without BLM treatment, and 10 cases with BLM treatment) were collected after clinical surgical resections at the Hospital of Stomatology, Wuhan University. All specimens were fixed in buffered 4% paraformaldehyde and embedded in paraffin. The procedures conform to the principles outlined in the Declaration of Helsinki. The study was approved by the review board of the Ethics Committee of the Hospital of Stomatology, Wuhan University. The diagnosis of venous malformation was established on the basis of pathological findings according to the classification system of vascular lesions proposed by Marler and Mulliken (2001).

Endothelial cell migration assay

Endothelial cell migration was detected by Transwell Boyden chamber assay (Becton-Dickinson, Franklin Lakes, NJ, USA).

Briefly, the medium containing a chemoattractant (VEGF, 5 ng·mL^{-1}) was added to the lower chambers, and then HUVECs (5×10^5) were suspended in 100 μL of serum-free EBM and seeded obto the upper chambers. After incubation at 37°C for 12 h, the migrated cells were fixed with methanol, stained with crystal violet, and then photographed and analysed.

Tube formation assay

HUVECs (2×10^5 cells) with or without BLM pretreatment were seeded onto 6 cm culture dishes coated with BD Matrigel™ Matrix (Becton-Dickinson) and incubated for 24 h at 37°C. After that, the formation of capillary-like structures was fixed and stained with PI, then observed using a fluorescence microscope (Leica, Solms, Germany); the tubes were scanned and counted using Image-Pro Plus 5.2 (Media Cybernetics, Silver Spring, MD, USA).

DNA fragmentation assay

The induction of apoptosis by BLM in HUVECs was determined by analysis of cytoplasmic histone-associated DNA fragmentation. Briefly, HUVECs at 1×10^4 per well were plated on 96-well plates and incubated with or without BLM for 72 h. Then, cytoplasmic histone-associated DNA fragmentation was determined with the cell death detection ELISA^{PLUS} kit (Roche Applied Science, Penzberg, Germany) according to the manufacturer's instructions.

Immunofluorescence analysis for cells

The localization of VE-cadherin and α-SMA was detected by indirect immunofluorescence analysis. In brief, HUVECs were grown on glass coverslips with indicated treatment. Then, cells were washed with PBS, fixed in 100% methanol at –20°C and blocked in 10% non-immune goat serum for 1 h at room temperature. After that, cells were incubated with the primary antibody indicated at a dilution of 1:200 overnight at 4°C followed by incubation with DyLight488-conjugated secondary antibody (1:400; Jackson Lab, West Grove, PA, USA) for 1 h at room temperature. The nuclei were stained with DAPI, and the coverslips were mounted on a microscope slide with embedding medium (Invitrogen, Carlsbad, CA, USA). The cells were observed and photographed with a fluorescence microscope (Leica).

Real-time quantitative PCR

Isolation of total RNA, synthesis of cDNA and real-time quantitative PCR were carried out as described previously (Sun *et al.*, 2010). Briefly, total RNA was isolated with TRIzol reagent (Invitrogen). Aliquots (1 μg) of RNA were reverse transcribed to cDNA (20 μL) with oligo(dT) and M-MuLV reverse transcriptase (Fermentas, Glen Burnie, MD, USA). One-fifth of the cDNA was used as a template for PCR using SYBR Premix Ex Taq™ (Perfect Real Time) kits (Takara, Kyoto, Japan) in an ABI 7500 real-time PCR system (Applied Biosystems, Foster City, CA, USA). GAPDH was selected as an internal control for each experiment. The primer nucleotide sequences for PCR are presented in Supporting Information Table S1.

Western blot analysis

The proteins in corresponding cells were collected, and the concentration of protein in supernatants was estimated using the BCA assay (Pierce, Rockford, IL, USA). Subsequently, 30 μg of protein was separated on 10% SDS-polyacrylamide gels and was electroblotted on PVDF membranes (Roche Applied Science). The blots were blocked overnight with 5% non-fat dry milk and probed with primary antibodies at dilutions recommended by the suppliers. Immunoblots were detected by HRP-conjugated secondary antibody (Pierce) using a chemiluminescence kit (Pierce) and photographed.

Statistical analysis

All values are expressed as the mean ± SEM of three independent experiments. Data analyses were conducted using OriginPro 8.6.0 (OriginLab Corporation, Northampton, MA, USA). One-way ANOVA and the Student–Newman–Keuls test were used for statistical analysis. $P < 0.05$ was considered statistically significant.

Results

BLM treatment induces EndoMT

Continuous BLM treatment for 72 h at 0.05 and 0.1 mU·mL^{-1} caused dramatic changes in HUVECs. The cell morphology was changed from a cobblestone-like shape to an elongated and spindle-shape (Figure 1A). Moreover, the intercellular adhesion molecule VE-cadherin, located at the borders of the control cells, was significantly down-regulated in the BLM-treated cells (Figure 1B and C). Correspondingly, an increase in α-SMA expression was observed in the treated group. Also, a decreased expression of CD31 and elevated levels of FSP-1 were confirmed by Western blot analysis (Figure 1C). Moreover, during the transformation the expressions of VE-cadherin, CD31 and CD34 mRNA were down-regulated, but the expressions of the mRNA of fibroblast markers, including α-SMA, FSP-1 and fibrosis proteins fibronectin and collagen I (Col I), were increased (Figure 1D and E). In addition, the size of the cells was enlarged and their protein content increased during the transformation (Figure 1F). Because an increase in cell size and protein content may also indicate cellular senescence (Hwang *et al.*, 2009), we also investigated this by performing β-galactosidase staining *in situ*; the results showed no obvious senescence in BLM-treated cells when compared with the control group (data not shown). Also, phalloidin–FITC staining showed that the cytoskeleton of BLM treated HUVECs was reorganized compared to the control cells (Figure 1G). All the above results strongly suggest that BLM treatment induces EndoMT.

BLM promotes endothelial cell migration but impaired tube formation

We next measured the functions of these transformed cells by transwell migration assays and tube formation assays respectively. The results revealed that the migration ability of these transformed cells was significantly enhanced (Figure 2A), but their ability to form and maintain networks were obviously weakened (Figure 2B).

Slug is the key transcription factor that mediates BLM-induced EndoMT

Considering the essential roles of transcription factors, including Twist, Snail and Slug, in EndoMT and EMT

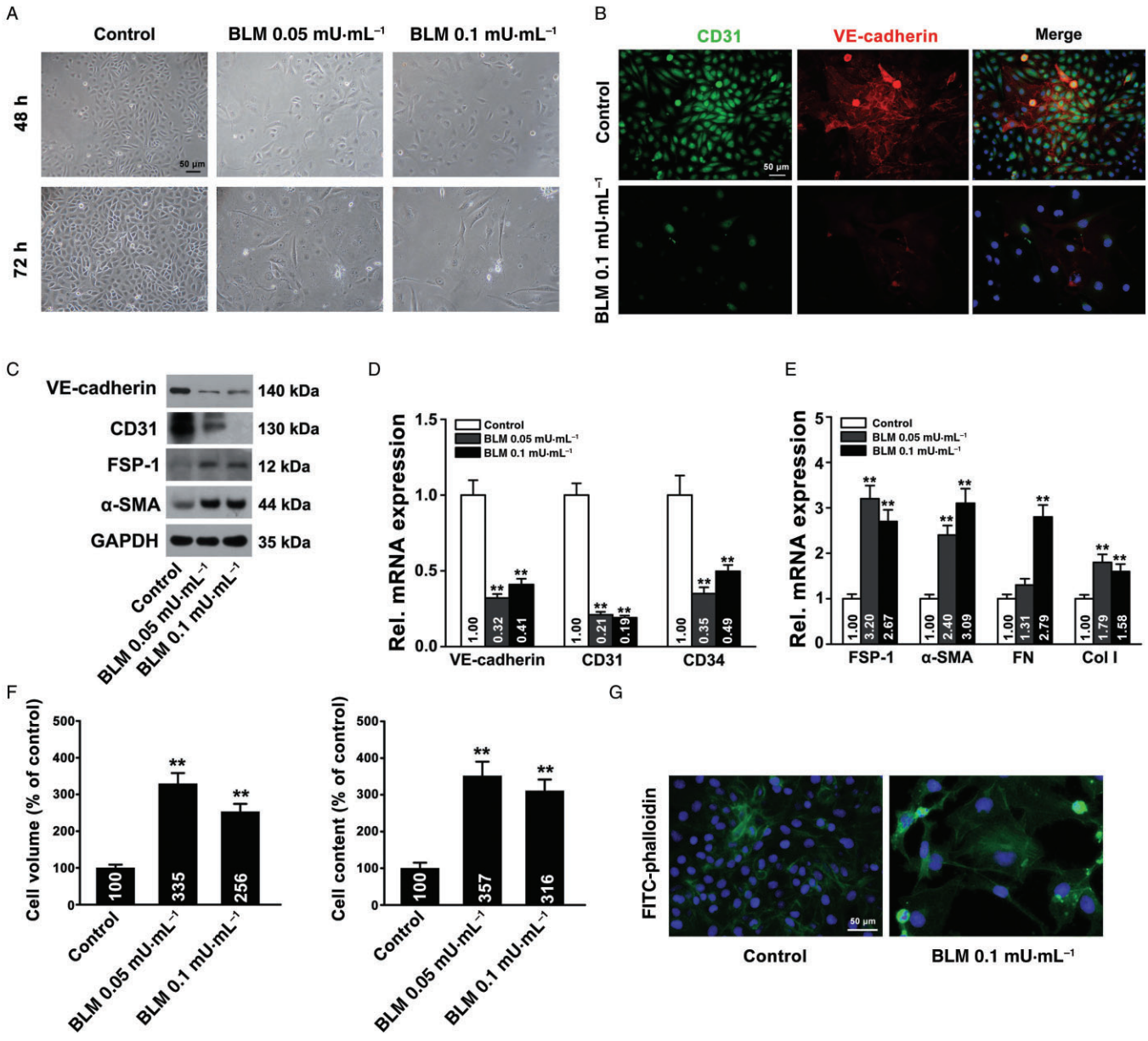

Figure 1

BLM induces EndoMT in HUVECs. (A) Spindle-shaped appearance of HUVECs after treatment with indicated concentrations of BLM at 48 and 72 h. (B) The down-regulation of VE-cadherin and up-regulation of α-SMA in BLM-treated HUVECs (0.1 mU·mL^{-1} for 72 h). (C) The down-regulation of VE-cadherin and CD31, and up-regulation of FSP-1 and α-SMA protein expression levels were detected in the BLM-treated HUVECs after 72 h. (D) The mRNA expression levels of VE-cadherin, CD31 and CD34 were down-regulated. (E) The mRNA expression levels of FSP-1, α-SMA, fibronectin and collagen I were up-regulated. (F) The enlarged cell size (left panel) and increased protein content (right panel), respectively, were also noted during the transformation. (G) Cytoskeleton changes during the transformation were visualized by staining of FITC-phalloidin (50 ng·mL^{-1}). The nuclei were stained by DAPI. The results of PCR are presented as a relative ratio to control group. The total or relative values for each quantitative analysis were labelled on the bar diagrams. All data are presented as mean ± SEM from three different experiments performed in duplicate. *P < 0.05; **P < 0.01 versus the control group.

(Piera-Velazquez *et al.*, 2011), the mRNA and protein expression levels of these transcription factors were then measured. Among the transcription factors tested, both the mRNA and protein levels of expression of Slug were found to be significantly increased, when compared with the slightly elevated expression of Snail and Twist (Figure 3A and B). In addition, the immunofluorescence analysis showed that amount of Slug located in the nucleus was increased in the BLM-treated endothelial cells (Figure 3C).

To validate the essential role of Slug in BLM-induced EndoMT, the expression of Slug was depleted by using a lentivirus siRNA against Slug (Figure 3D). The Slug-depleted HUVECs retained their cobblestone-like shape after BLM treatment, but did not transform to a fibroblast-like

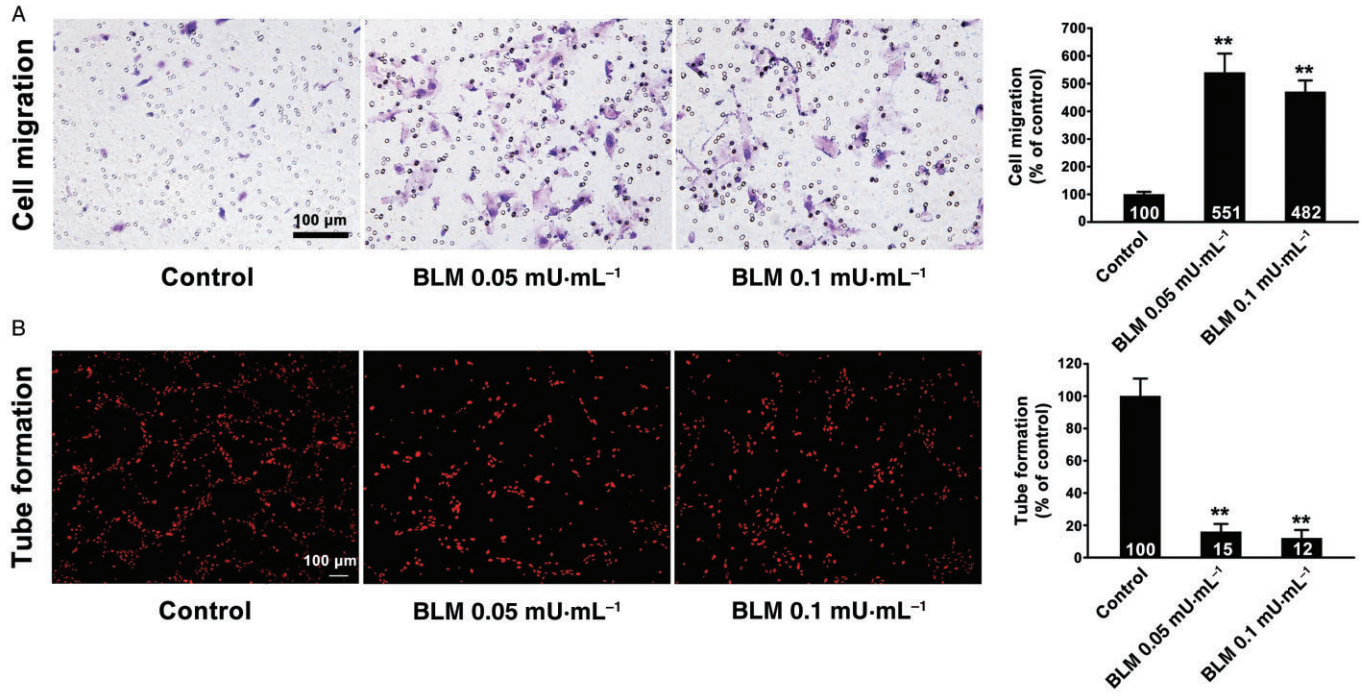

Figure 2

BLM promotes endothelial cell migration but impairs tube formation. (A) The enhanced cell migration was determined by transwell migration assays. The numbers of migrated cells were quantified in the right panel. (B) The weakened formation of capillary-like structures was measured by tube formation assays. The formation of capillary-like structures was analysed relative to the control group. The total or relative values for each quantitative analysis are labelled on the bar diagrams. All data are presented as mean ± SEM from three different experiments performed in duplicate. *$P < 0.05$; **$P < 0.01$ versus the control group.

appearance (Figure 3E). Also, the down-regulation of VE-cadherin and up-regulation of α-SMA were not detected in the Slug-depleted cells treated with BLM for 72 h; this was further confirmed by Western blot analyses and immunocytofluorescence assays (Figure 3D and E). However, knockdown of Slug did not prevent the increase in cell size and protein content induced by BLM treatment indicating that other mechanisms are involved. In summary, we demonstrated that Slug, a member of zinc finger transcription factors family, played an essential role in BLM-induced EndoMT.

BLM-mediated EndoMT is not due to the induction of apoptosis

Even low concentrations of BLM were shown to have apoptotic effects on HUVECs (Figure 4A). It has been reported that apoptotic endothelial cells induced by BLM could secrete connective tissue growth factor (CTGF), a cytokine that induces an EMT-like process in a caspase-dependent manner (Laplante *et al.*, 2010; Jiang *et al.*, 2013). Consistently, an increased expression of CTGF was also observed in our present study by quantitative real-time PCR (Figure 4A). To investigate a possible role of secreted CTGF in the transformation of these cells, Z-VAD-FMK, a pan inhibitor of caspases, was used to block the production of this cytokine (Figure 4B). Z-VAD-FMK did not affect the reduction in VE-cadherin induced by BLM treatment (Figure 4C). The immunofluorescence assays also demonstrated that Z-VAD-FMK failed to affect the morphology of the BLM-treated cells or their expression of α-SMA or VE-cadherin (Figure 4D). Therefore, we concluded that BLM-mediated EndoMT is not due to the induction of apoptosis and CTGF secretion.

The Akt/mTOR pathway is involved in BLM-induced EndoMT

Previous studies have indicated that the function of Slug can be modulated by several signalling pathways, including the Akt pathway (Lau and Leung, 2012). Hence, we determined the activation of the Akt signalling pathway by Western blot analysis and showed that the activation of Akt and its downstream signals mTOR and S6 was upregulated in the BLM-treated transformed cells (Figure 5A). Next, rapamycin (100 nM), a specific inhibitor of mTOR, was used to validate the role of mTOR in BLM-induced EndoMT. As shown (Figure 5B), after inhibition of the mTOR pathway by rapamycin, BLM failed to transform HUVECs; this was confirmed by the immunofluorescence analysis (Figure 5C). The Western blot analysis also revealed that the expression of VE-cadherin was maintained at a high level, and the increase in α-SMA expression was also prevented in the rapamycin-treated cells (Figure 5B). Rapamycin also prevented the increase in cell size and protein content induced by BLM. In addition, the cell apoptosis induced by BLM was enhanced in rapamycin-treated cells, manifested as an enhanced cleavage of caspase 3

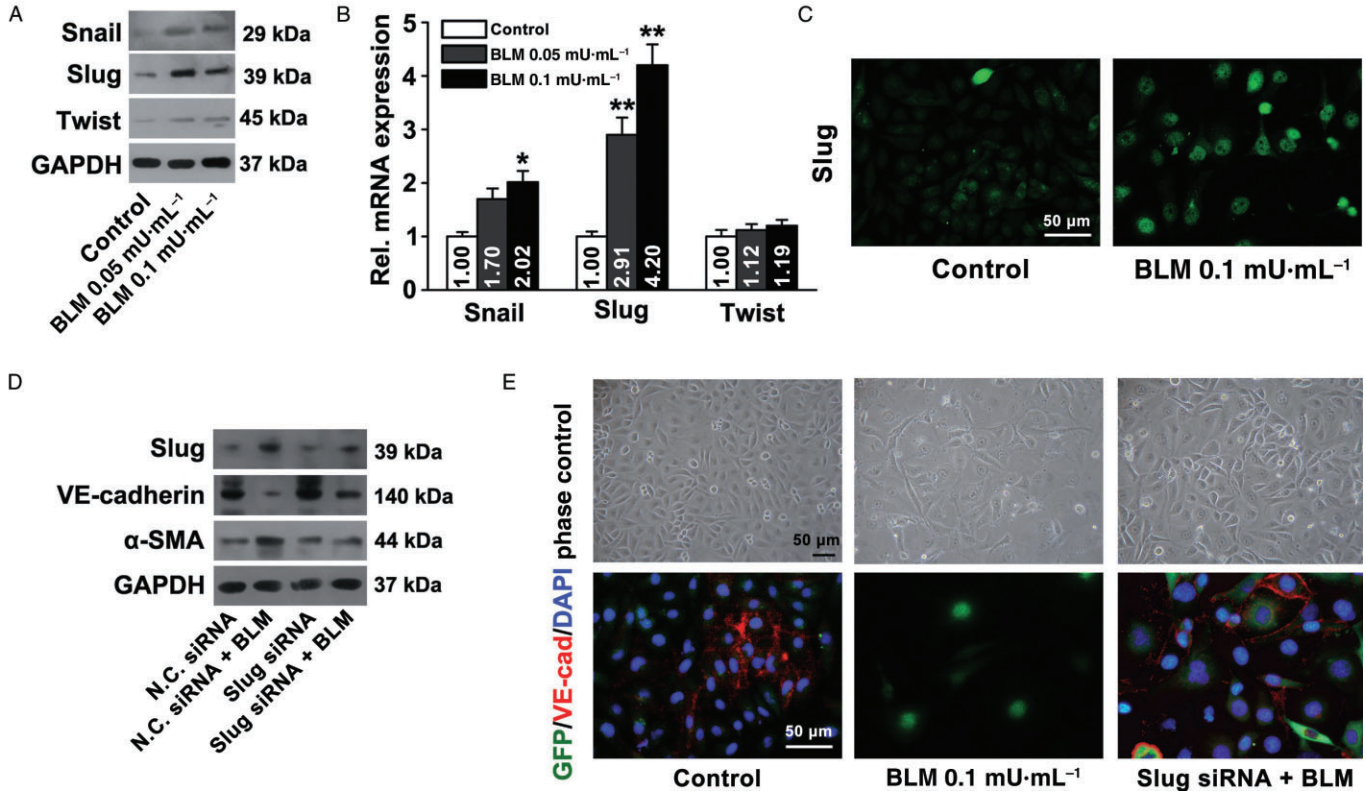

Figure 3

Slug is the key transcription factor that mediates BLM-induced EndoMT. (A) The increased protein expression levels of Snail, Slug and Twist were analysed by Western blot. (B) The increased mRNA expression levels of Snail and Slug (but not Twist) were measured by quantitative real-time PCR. (C) Nuclear location of Slug was detected by immunofluorescence analysis. (D) The depletion of Slug using RNA interference prevented the reduction in VE-cadherin and up-regulation of α-SMA in the BLM-treated cells. (E) Morphological changes and the VE-caderin expression and localization were analysed by immunofluorescence. The results of PCR are presented as relative ratio to the control group. The total or relative values for each quantitative analysis are labelled on the bar diagrams. All data are presented as mean ± SEM from three different experiments performed in duplicate. *$P < 0.05$; **$P < 0.01$ versus the control group.

(Figure 5B). Cell migration and tube formation were also measured after rapamycin treatment, and it was found that the enhanced migration was significantly reversed by rapamycin, although tube formation was still diminished (Figure 5D and E). All of the above findings suggested that the Akt/mTOR pathway plays an important role in BLM-induced EndoMT.

Slug was detected in BLM-treated venous malformations

For clinical significance, we next investigated whether BLM treatment could induce EndoMT in human VM samples. The specimens of VMs with or without BLM treatment were collected and the expression levels of CD34, α-SMA and Slug were measured using immunohistochemistry. Representative immunohistochemical results for the cases selected are shown in Figure 6. Histologically, compared with untreated lesions, the VMs treated with BLM showed decreased venous lumen and thickened lumen walls composed of multilayer shaped cells. Also, in most of BLM-treated VMs, the abnormal venous channels were inapparent or smaller, whereas the thickness of the mesenchymal tissue between channels was significantly increased in BLM-treated VMs. From the immunohistochemistry, in the untreated group, the expression of CD34 was demonstrated to be continuous and localized at the intima of the vessels, whereas in most of the BLM-treated cases, the continuous expression of CD34 was damaged and replaced by increased expression of α-SMA around the vessels, which had even invaded the endothelial layers. Most importantly, the nuclear location of Slug was observed in the inner layer of the vessels in most of BLM-treated VM samples (6/10), compared with the negative staining of Slug in all untreated lesions (0/10), suggesting the occurrence of EndoMT.

Discussion and conclusions

Previous studies have indicated that BLM, one of the most common sclerosants used to treat VM, invariably causes fibrosis of the lesions (Dompmartin *et al.*, 2010). BLM not only induces the apoptosis of endothelial cells but also causes dramatic changes in the expression of adhesion molecules (Horikawa *et al.*, 2006). The expression of E-selectin, one of the adhesion molecules that regulates the homing of lymphocytes in acute inflammation, was found to be upregulated

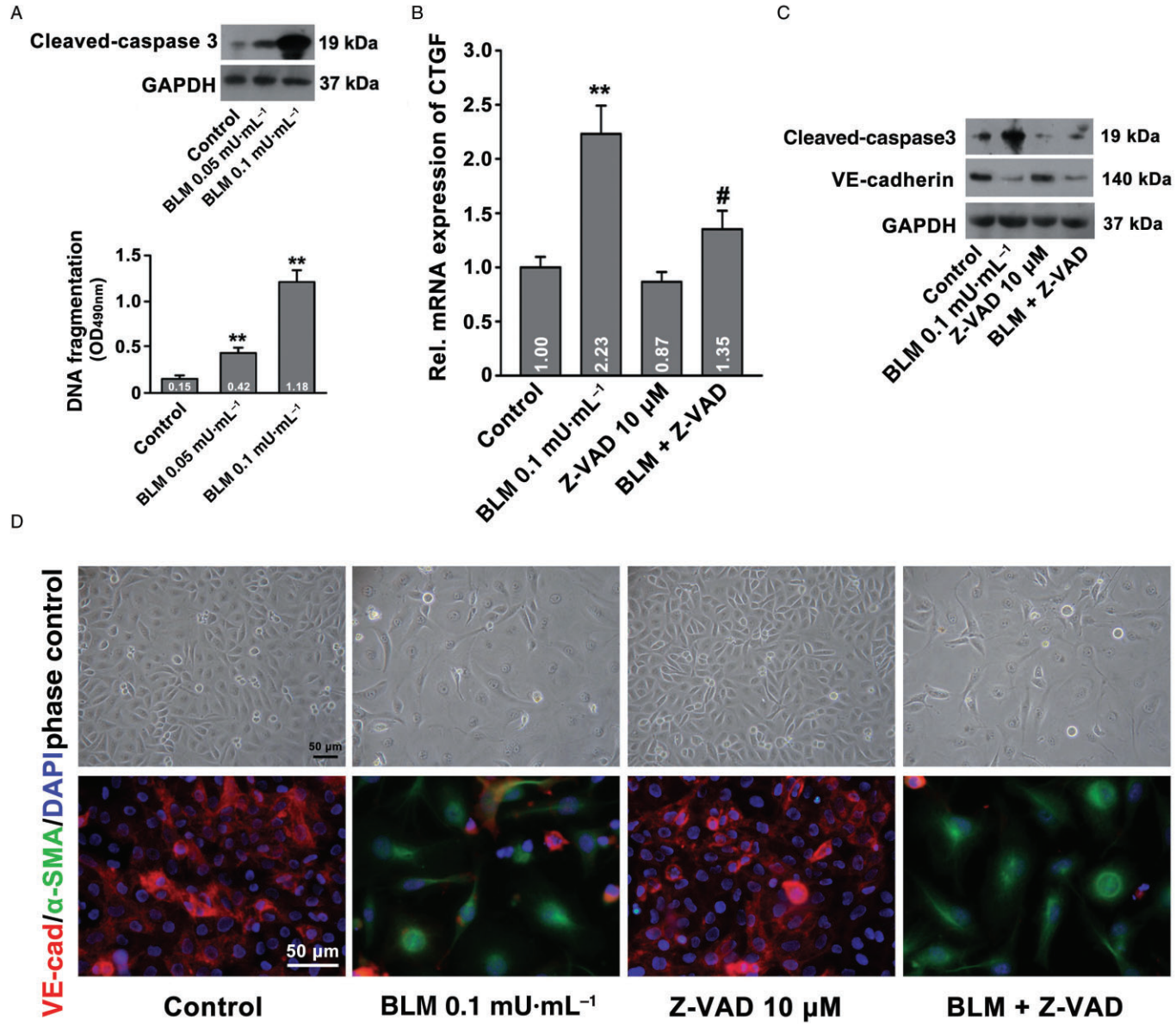

Figure 4

BLM-mediated EndoMT is not due to the enhanced induction of apoptosis. (A) An increased expression of cleaved-caspase 3 was determined in HUVECs treated with BLM (0.1 mU·mL^{-1}) for 72 h (top panel), and an augmentation of DNA fragmentation of BLM-treated HUVECs was observed after BLM treatment (lower panel). (B) The relative expression of CTGF mRNA in HUVECs induced after BLM treatment. HUVECs were treated with BLM at a concentration of 0.1 mU·mL^{-1} for 72 h in the presence of Z-VAD-FMK (Z-VAD, 10 μM). (C) Z-VAD suppressed the activity of caspase 3 but showed no effect on the expression level of VE-cadherin protein. (D) Morphological changes and immunofluorescent staining of VE-cadherin and α-SMA were also detected. The total or relative values for each quantitative analysis are labelled on the bar diagrams. All data are presented as mean ± SEM from three different experiments performed in duplicate. *P < 0.05; **P < 0.01 versus the control group; #P < 0.05 versus BLM-treated group.

in BLM-treated endothelial cells (Horikawa *et al.*, 2006). In addition, BLM is also widely used as an inducer of pulmonary fibrosis in rodent models, and the effect of BLM on endothelial cells has been studied in these models. Furthermore, in an *in vitro* study focusing on the effects of BLM on bovine pulmonary artery endothelial cells, it was shown that BLM induces cytoskeleton re-arrangement and alterations in the levels of tight junction proteins, such as ZO-1 and claudins (Ohta *et al.*, 2012), which are considered to play important roles in maintaining the morphology of these cells and regulating permeability (Feng *et al.*, 2011). It has also been noted that during BLM-induced pulmonary fibrosis, endothelial cells can change into fibroblasts by a transformation process known as EndoMT (Hashimoto *et al.*, 2010). However, the precise mechanisms underlying BLM-induced EndoMT are yet to be elucidated. In the present study, we showed that

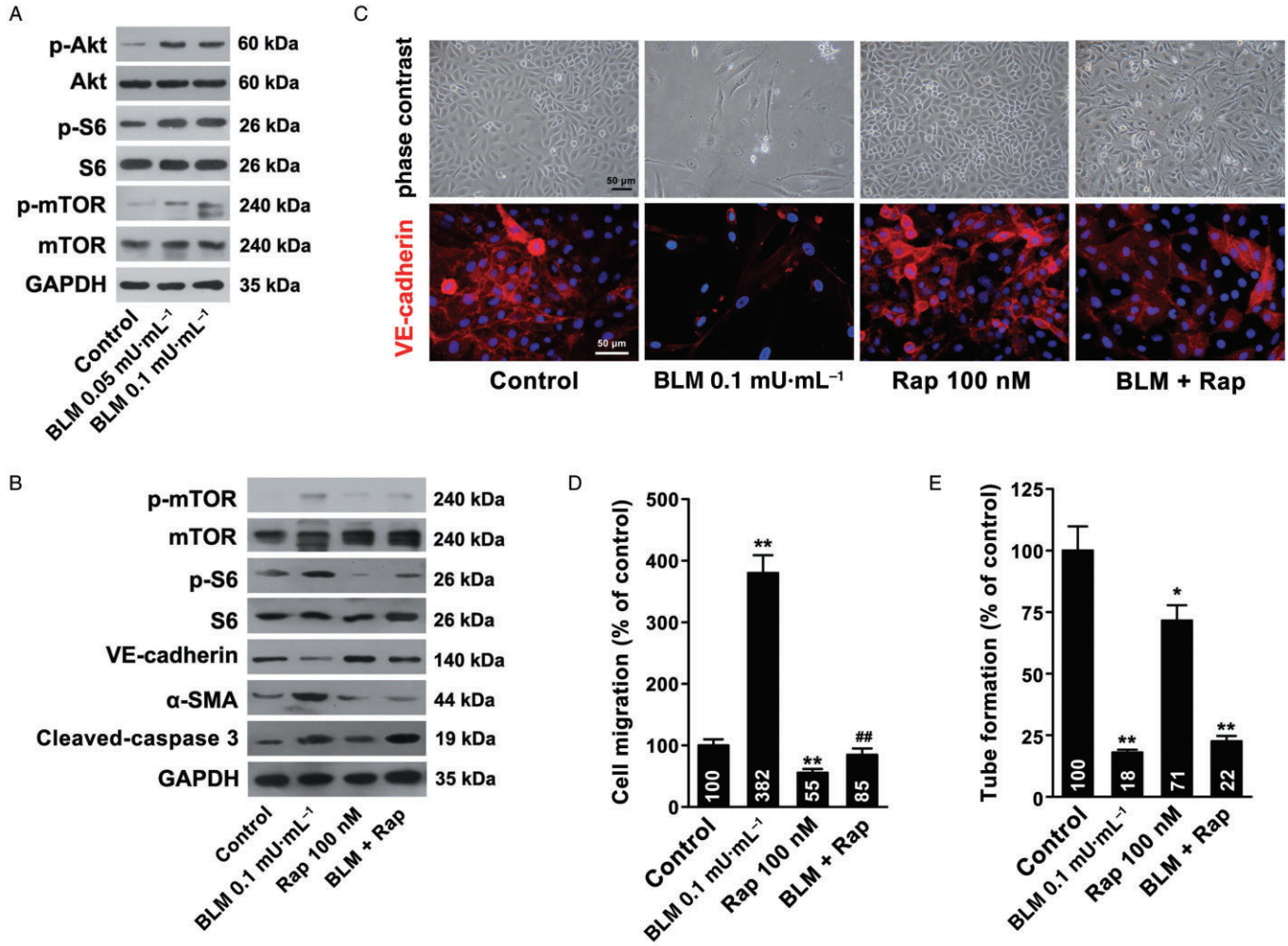

Figure 5

The Akt/mTOR pathway is involved in BLM-induced EndoMT. (A) The expressions of Akt, p-Akt, mTOR, p-mTOR, S6 and p-S6 proteins in HUVECs after BLM treatment (0.1 mU·mL^{-1} for 72 h) were increased. (B) Rapamycin (Rap, 100 nM) prevented the increased expression of p-mTOR, mTOR, p-S6, S6 and α-SMA , restored the expression of VE-cadherin suppressed by BLM (0.1 mU·mL^{-1} for 72 h), but showed no obvious effects on the expression of cleaved-caspase 3. (C) Rapamycin prevented BLM-induced morphological changes and VE-cadherin suppression. (D) Rapamycin inhibited the enhanced cell migration of HUVECs induced by BLM, and a quantitative analysis was performed. (E) The formation of capillary-like structures was measured by tube formation assays, and quantitative analysis was performed. The total or relative values for each quantitative analysis are labelled on the bar diagrams. All data are presented as mean ± SEM from three different experiments performed in duplicate. *P < 0.05; **P < 0.01 versus the control group; ##P < 0.01 versus BLM-treated group.

BLM treatment induced endothelial cells to undergo an EndoMT-like process in an mTOR-dependent manner, and showed that Slug is likely to be involved in this process. More importantly, we also revealed the EndoMT-like process in BLM-treated VM samples from patients. To our knowledge, this study is the first to implicate the EndoMT-like process in the sclerotherapy of VMs.

EndoMT is a process by which endothelial cells lose their endothelial characteristics and gain those of fibroblast. During this process, endothelial markers such as CD31 and VE-cadherin are down-regulated, whereas the expression of fibroblasts markers, which include FSP-1 and α-SMA, are significantly up-regulated (Piera-Velazquez *et al.*, 2011). EndoMT was first shown to occur during embryonic pulmonary artery development where the cells are involved in intimal formation and in pulmonary vascular remodelling (Arciniegas *et al.*, 2005). There is also evidence suggesting that EndoMT may play an important role in the development of renal, pulmonary and cardiac fibrosis in several pathological conditions (Harrison and Lazo, 1987; Muir *et al.*, 2004; Li *et al.*, 2010). Similar to EMT, the TGF-β signalling pathway has also been shown to have an important role in EndoMT (Koitabashi *et al.*, 2011; Yoshimatsu and Watabe, 2011). TGF-β2, but not TGF-β1, is considered to be a strong inducer of EndoMT (Medici *et al.*, 2011). In addition, several signalling pathways have been shown to be involved in TGF-β2-mediated EndoMT, including Smad, MAPK/ERK, PI3K and p38 MAPK (Medici *et al.*, 2011). In the present study, the

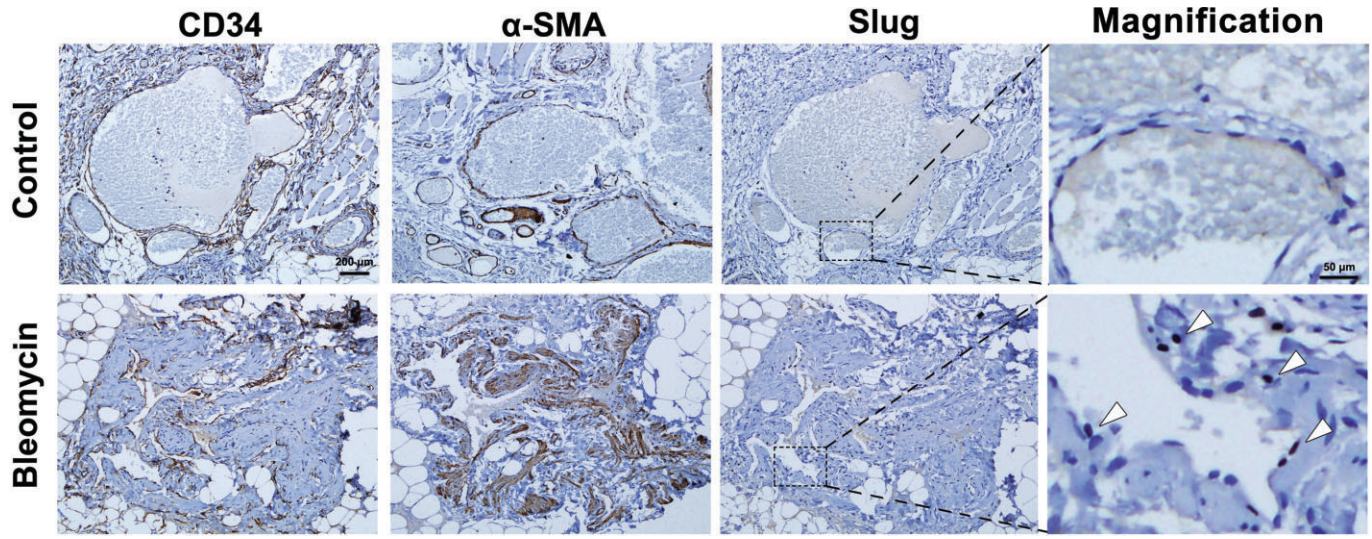

Figure 6

Expression levels of CD34, α-SMA and Slug in human VMs. Representative immunohistochemical staining of CD34, α-SMA and Slug in human VM specimens with or without BLM treatment (10 samples respectively). The VMs treated with BLM showed decreased venous lumen and thickened lumen walls composed of multilayers of shaped cells. Meanwhile, in the BLM-treated samples, the continuous expression of CD34 was damaged and replaced by increased expression of α-SMA around the vessels, and α-SMA had even invaded across the endothelial layers; the nuclear location of Slug (6/10) was observed in the inner cells of the lumen in BLM-treated VMs.

corresponding inhibitors for these pathways were used to explore their involvement in BLM-induced EndoMT. Our results excluded the participation of MAPK signalling pathways and confirmed that mTOR, one of the most important downstream signals of the PI3K/Akt pathway, has an essential role in the BLM-induced EndoMT. This is consistent with recent findings where it was shown that BLM activates the Akt/mTOR signalling pathway and stimulates the synthesis of ECM proteins by fibroblasts (Goc *et al.*, 2011), indicating the importance of Akt/mTOR pathway in fibrogenic events. In a previous study it was suggested that during BLM-induced apoptosis (Laplante *et al.*, 2010), CTGF, an inducer of EMT and fibrosis, is significantly up-regulated in a caspase-dependent manner (Jiang *et al.*, 2013), therefore, we determined the potential involvement of apoptotic endothelial cells in BLM-induced EndoMT. By using Z-VAD-FMK, a pan inhibitor of caspases that significantly decreased the expression of CTGF in BLM-treated endothelial cells, we concluded that BLM-mediated EndoMT is not due to the increased induction of apoptosis and CTGF secretion.

Rapamycin has been demonstrated to prevent interstitial, cardiac and pulmonary fibrosis in animal models (Korfhagen *et al.*, 2009; Yu *et al.*, 2013). Moreover, in a skin fibrosis model, treatment with rapamycin was effective at reducing the thickness of skin during the fibrotic process induced by BLM (Yoshizaki *et al.*, 2010). This reduction in fibrosis caused by rapamcyin was considered to be associated with its ability to reduce inflammation (Tulek *et al.*, 2011). However, there is now increasing evidence that rapamycin and its derivatives induce their effects through specific inhibition of mTOR (Lian *et al.*, 2012). Moreover, the Akt/mTOR pathway is usually activated during the EMT process, especially in the presence of cytokines, such as TGF-β and EGF (Lamouille and Derynck, 2007; Sabbah *et al.*, 2008). Previous studies have suggested that several EMT-related transcription factors could be regulated by mTOR, including Snail and Slug (Lamouille *et al.*, 2012; Palma-Nicolás and López-Colomé, 2013). By promoting the biosynthesis of transcription factors, mTOR participates in the regulation of these factors. In our experiments, it was noticed that rapamycin significantly down-regulated the expression of Slug, as demonstrated by the ability of rapamycin to prevent the BLM-induced transformation of cell phenotype (Ruvinsky and Meyuhas, 2006).

It is well known that BLM is in contact with the intimal endothelial cells during intralesional sclerotherapy with BLM. Consistently, the number of fibroblasts positive for α-SMA, as detected histologically, was shown to be increased in BLM-treated VM tissues compared with untreated tissues. Most importantly, a positive nuclear location of Slug was obviously apparent in the intima of most of the BLM-treated VM specimens, suggesting that the fibroblasts arising in the treated tissue partially originate from endothelial cells, consistent with previous reports regarding BLM-induced pulmonary fibrosis models (Hashimoto *et al.*, 2010).

Taken together, our results demonstrate, for the first time, the possible involvement of Slug-dependent EndoMT in BLM-induced therapeutic effects in endothelial cells and, more importantly, indicate its potential role in the sclerotherapy of VMs. Specific targeting of the EndoMT-like process could further advance the development of novel sclerosants.

Acknowledgements

This work was supported by the National Natural Science Foundation of China (81170977, 81371159, 81300895) and the Fundamental Research Funds for the Central Universities (2012304020203).

Conflict of interest

None.

References

Arciniegas E, Neves CY, Carrillo LM, Zambrano EA, Ramirez R (2005). Endothelial–mesenchymal transition occurs during embryonic pulmonary artery development. Endothelium 12: 193–200.

Dompmartin A, Vikkula M, Boon LM (2010). Venous malformation: update on aetiopathogenesis, diagnosis and management. Phlebology 25: 224–235.

Feng S, Cen J, Huang Y, Shen H, Yao L, Wang Y *et al.* (2011). Matrix metalloproteinase-2 and -9 secreted by leukemic cells increase the permeability of blood–brain barrier by disrupting tight junction proteins. PLoS ONE 6: e20599.

Goc A, Choudhary M, Byzova TV, Somanath PR (2011). TGFbeta- and bleomycin-induced extracellular matrix synthesis is mediated through Akt and mammalian target of rapamycin (mTOR). J Cell Physiol 226: 3004–3013.

Harrison JH, Jr, Lazo JS (1987). High dose continuous infusion of bleomycin in mice: a new model for drug-induced pulmonary fibrosis. J Pharmacol Exp Ther 243: 1185–1194.

Hashimoto N, Phan SH, Imaizumi K, Matsuo M, Nakashima H, Kawabe T *et al.* (2010). Endothelial–mesenchymal transition in bleomycin-induced pulmonary fibrosis. Am J Respir Cell Mol Biol 43: 161–172.

Horikawa M, Fujimoto M, Hasegawa M, Matsushita T, Hamaguchi Y, Kawasuji A *et al.* (2006). E- and P-selectins synergistically inhibit bleomycin-induced pulmonary fibrosis. Am J Pathol 169: 740–749.

Hwang ES, Yoon G, Kang HT (2009). A comparative analysis of the cell biology of senescence and aging. Cell Mol Life Sci 66: 2503–2524.

Jia J, Zhang W, Liu JY, Chen G, Liu H, Zhong HY *et al.* (2012). Epithelial mesenchymal transition is required for acquisition of anoikis resistance and metastatic potential in adenoid cystic carcinoma. PLoS ONE 7: e51549.

Jiang CG, Lv L, Liu FR, Wang ZN, Na D, Li F *et al.* (2013). Connective tissue growth factor is a positive regulator of epithelial–mesenchymal transition and promotes the adhesion with gastric cancer cells in human peritoneal mesothelial cells. Cytokine 61: 173–180.

Koitabashi N, Danner T, Zaiman AL, Pinto YM, Rowell J, Mankowski J *et al.* (2011). Pivotal role of cardiomyocyte TGF-beta signaling in the murine pathological response to sustained pressure overload. J Clin Invest 121: 2301–2312.

Korfhagen TR, Le Cras TD, Davidson CR, Schmidt SM, Ikegami M, Whitsett JA *et al.* (2009). Rapamycin prevents transforming growth factor-alpha-induced pulmonary fibrosis. Am J Respir Cell Mol Biol 41: 562–572.

Lamouille S, Derynck R (2007). Cell size and invasion in TGF-beta-induced epithelial to mesenchymal transition is regulated by activation of the mTOR pathway. J Cell Biol 178: 437–451.

Lamouille S, Connolly E, Smyth JW, Akhurst RJ, Derynck R (2012). TGF-beta-induced activation of mTOR complex 2 drives epithelial–mesenchymal transition and cell invasion. J Cell Sci 125 (Pt 5): 1259–1273.

Laplante P, Sirois I, Raymond MA, Kokta V, Beliveau A, Prat A *et al.* (2010). Caspase-3-mediated secretion of connective tissue growth factor by apoptotic endothelial cells promotes fibrosis. Cell Death Differ 17: 291–303.

Lau MT, Leung PC (2012). The PI3K/Akt/mTOR signaling pathway mediates insulin-like growth factor 1-induced E-cadherin down-regulation and cell proliferation in ovarian cancer cells. Cancer Lett 326: 191–198.

Li J, Qu X, Yao J, Caruana G, Ricardo SD, Yamamoto Y *et al.* (2010). Blockade of endothelial–mesenchymal transition by a Smad3 inhibitor delays the early development of streptozotocin-induced diabetic nephropathy. Diabetes 59: 2612–2624.

Lian H, Ma Y, Feng J, Dong W, Yang Q, Lu D *et al.* (2012). Heparin-binding EGF-like growth factor induces heart interstitial fibrosis via an Akt/mTor/p70s6k pathway. PLoS ONE 7: e44946.

McRae MY, Adams S, Pereira J, Parsi K, Wargon O (2013). Venous malformations: clinical course and management of vascular birthmark clinic cases. Australas J Dermatol 54: 22–30.

Marler JJ, Mulliken JB (2001). Vascular anomalies: classification, diagnosis, and natural history. Facial Plast Surg Clin North Am 9: 495–504.

Medici D, Potenta S, Kalluri R (2011). Transforming growth factor-beta2 promotes Snail-mediated endothelial–mesenchymal transition through convergence of Smad-dependent and Smad-independent signalling. Biochem J 437: 515–520.

Mouratis MA, Aidinis V (2011). Modeling pulmonary fibrosis with bleomycin. Curr Opin Pulm Med 17: 355–361.

Muir T, Kirsten M, Fourie P, Dippenaar N, Ionescu GO (2004). Intralesional bleomycin injection (IBI) treatment for haemangiomas and congenital vascular malformations. Pediatr Surg Int 19: 766–773.

Odeyinde SO, Kangesu L, Badran M (2013). Sclerotherapy for vascular malformations: complications and a review of techniques to avoid them. J Plast Reconstr Aesthet Surg 66: 215–223.

Ohta H, Chiba S, Ebina M, Furuse M, Nukiwa T (2012). Altered expression of tight junction molecules in alveolar septa in lung injury and fibrosis. Am J Physiol Lung Cell Mol Physiol 302: L193–L205.

Palma-Nicolás JP, López-Colomé AM (2013). Thrombin induces slug-mediated E-cadherin transcriptional repression and the parallel up-regulation of N-cadherin by a transcription-independent mechanism in RPE cells. J Cell Physiol 228: 581–589.

Piera-Velazquez S, Li Z, Jimenez SA (2011). Role of endothelial–mesenchymal transition (EndoMT) in the pathogenesis of fibrotic disorders. Am J Pathol 179: 1074–1080.

Ruvinsky I, Meyuhas O (2006). Ribosomal protein S6 phosphorylation: from protein synthesis to cell size. Trends Biochem Sci 31: 342–348.

Sabbah M, Emami S, Redeuilh G, Julien S, Prevost G, Zimber A *et al.* (2008). Molecular signature and therapeutic perspective of the epithelial-to-mesenchymal transitions in epithelial cancers. Drug Resist Updat 11: 123–151.

Sun ZJ, Cai Y, Chen G, Wang R, Jia J, Chen XM *et al.* (2010). LMO2 promotes angiogenesis probably by up-regulation of bFGF in endothelial cells: an implication of its pathophysiological role in infantile haemangioma. Histopathology 57: 622–632.

Thiery JP, Acloque H, Huang RY, Nieto MA (2009). Epithelial–mesenchymal transitions in development and disease. Cell 139: 871–890.

Tulek B, Kiyan E, Toy H, Kiyici A, Narin C, Suerdem M (2011). Anti-inflammatory and anti-fibrotic effects of sirolimus on bleomycin-induced pulmonary fibrosis in rats. Clin Invest Med 34: E341.

Wouters V, Limaye N, Uebelhoer M, Irrthum A, Boon LM, Mulliken JB *et al*. (2010). Hereditary cutaneomucosal venous malformations are caused by TIE2 mutations with widely variable hyper-phosphorylating effects. Eur J Hum Genet 18: 414–420.

Yamamoto T, Katayama I (2011). Vascular changes in bleomycin-iduced scleroderma. Int J Rheumatol 2011. doi: 10.1155/2011/270938.

Yoshimatsu Y, Watabe T (2011). Roles of TGF-beta signals in endothelial–mesenchymal transition during cardiac fibrosis. Int J Inflamm 2011. doi: 10.4061/2011/724080.

Yoshizaki A, Yanaba K, Iwata Y, Komura K, Ogawa F, Takenaka M *et al*. (2010). Treatment with rapamycin prevents fibrosis in tight-skin and bleomycin-induced mouse models of systemic sclerosis. Arthritis Rheum 62: 2476–2487.

Yu SY, Liu L, Li PU, Li J (2013). Rapamycin inhibits the mTOR/p70S6K pathway and attenuates cardiac fibrosis in adriamycin-induced dilated cardiomyopathy. Thorac Cardiovasc Surg 61: 223–228.

Zeisberg EM, Tarnavski O, Zeisberg M, Dorfman AL, McMullen JR, Gustafsson E *et al*. (2007). Endothelial-to-mesenchymal transition contributes to cardiac fibrosis. Nat Med 13: 952–961.

Zou HX, Jia J, Zhang WF, Sun ZJ, Zhao YF (2013). Propranolol inhibits endothelial progenitor cell homing: a possible treatment mechanism of infantile hemangioma. Cardiovasc Pathol 22: 203–210.

Supporting information

Additional Supporting Information may be found in the online version of this article at the publisher's web-site:

http://dx.doi.org/10.1111/bph.12355

Table S1. Primer sequences used for real-time quantitative PCR.